Geosynthetics, J. Kuwano & J. Koseki (eds)

Deformation of geosynthetic-reinforced clay subjected to wetting-drying

Pathak, Y.P. & Alfaro, M.C.
Department of Civil Engineering, University of Manitoba, Winnipeg, Canada

Keywords: reinforced clay, embankment, deformation, wetting-drying, geosynthetics

ABSTRACT: Results from laboratory model tests and numerical analysis are presented to assess the effect of wetting-drying on geogrid-reinforced clay. Wetting-drying induced deformations of clay specimen and geogrid strains were measured in the laboratory. Numerical analysis was also carried out to develop the understanding of deformation of the reinforced clay under wetting condition. User defined constitutive models which represent the wetting effects on expansive clay were written in a finite-difference program, Fast Lagrangian Analysis of Continuum (FLAC). Numerical results are compared here with the laboratory model test results which show reasonably good comparison.

1 INTRODUCTION

Granular soils are often recommended as an ideal fill in geosynthetic-reinforced soil (GRS) structures. Consequently, the economic benefits of the GRS structures are largely limited by the availability and cost of imported granular fill. Cost savings could potentially be realized by using on-site native soils which are mostly fine-grained soils as in the case of Manitoba where clays and silts are readily available. However, clays in Manitoba are generally expansive and silts are frost susceptible. When considering the use of expansive clays as reinforced fills, environmental effects (swell-shrink) become an important consideration in the performance of the GRS structures.

Few laboratory investigations are found in literature to explore the possibility of geosynthetic inclusion for reducing swelling of expansive clays (Al-Omari and Hamodi 1991, Vessely and Wu 2002). In this paper, wetting-drying tests were performed in the laboratory on compacted clay specimen reinforced with geogrid. Reinforcement strains and deformations within the reinforced soil specimen were monitored. Geogrid reinforcement was placed at the middle of specimen during specimen preparation. Tests were conducted at plane-strain condition with independently applied constant horizontal and vertical pressures. Wetting-drying were simulated by flooding the specimen with water and then, subsequently removing water and supplying hot air to the specimen. Numerical analysis was also performed to simulate the wetting condition in the laboratory specimen. Laboratory and numerical analysis results are compared.

2 LABORATORY TEST

2.1 *Test materials*

Soil used in this study is locally available Winnipeg clay. Soil has following basic properties: specific gravity = 2.72, liquid limit = 96%, plastic limit = 35%, maximum dry unit weight = 13.3 kN/m^3 and optimum moisture content = 30%. Soil contains more than 95% of particles passing No. 200 sieve. It is classified as high plastic clay (CH) based on Unified Soil Classification System (USCS). An extruded biaxial polypropylene geogrid designated as BX1300 from Tensar Earth Technology Inc. has been used as reinforcement specimen. Virgin BX1300 was modified in this study to create weaker reinforcement by removing every alternate rib in the cross machine direction so that reasonable strains can be measured in the geogrid during the wetting-drying of the reinforced clay block.

2.2 *Test set-up and instrumentations*

Laboratory test was designed in this study to simulate wetting-drying effect in the geosynthetic-reinforced clay. A large unit cell test apparatus was developed and commissioned at the University of Manitoba for this purpose. Geosynthetic-reinforced clay block (500 mm (H) × 420 mm (L) × 430 mm (B)) was prepared and tested in this apparatus under anisotropic stress and plane-strain condition. Details of the apparatus, test set-up, specimen preparation and testing procedures have been described in Pathak and Alfaro (2005). Brief description of test set-up and testing programs are given below.

Geogrid-reinforced clay specimen (Figure 1) was prepared by compacting clay at optimum moisture-maximum dry density. Geogrid (with strain gauges attached) and psychrometers were embedded in the test specimen during the specimen preparation. Four linear position sensors (LPS) were attached at positions L_T and L_B to measure the lateral deformations of the test block. Linear variable displacement transducer (LVDT) was installed on top of the specimen to measure vertical displacement. Psychrometers were used to measure suction in the clay and thus, moisture content or saturation during the test. Soil specimen has 450 kPa of total suction (corresponding degree of saturation = 80%) at its compacted condition before wetting. Three pairs of strain gauges (S_1, S_2 and S_3) were attached in the geogrid to measure the geogrid strain. Plane-strain condition was subjected in the test specimen by restraining the deformation of sample in z-direction (i.e perpendicular to the plane of paper in Figure 1).

Prepared sample was first applied with incremental stresses up to desired stress levels (mechanical loading) at its compacted condition before subjecting wetting-drying to simulate environmental loading. Both vertical pressure (σ_y) and horizontal pressure (σ_x) were applied independently. Vertical pressure was applied via loading ram on top of the specimen and horizontal pressure was applied on the sides of specimen through flexible air bags. This loading condition was continued until equilibrium deformation was reached. The test box was then flooded by supplying water to simulate wetting condition in the clay. Once full swell was achieved at about full saturation, water from the test box was removed. The clay specimen was then dried by supplying hot air pressure at 35°C to 40°C from bottom and top of the test specimen (the reinforced clay specimen was found to have a maximum temperature of 25°C). Drying was observed to be a very slow process and was interrupted due to time constraint before sample shrinkage reached the equilibrium condition. All the monitoring instrumentations were connected with data acquisition system and data were monitored and recorded electronically.

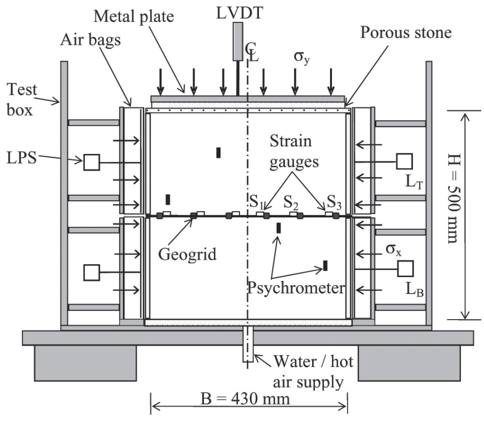

Figure 1. Schematic of test apparatus and geogrid-reinforced clay specimen with layout of instrumentations.

2.3 *Laboratory test results and discussions*

Series of test were conducted at different stress level. Here, test results of stress level: σ_y = 20 kPa and σ_x = 14 kPa are presented and this stress level is denoted as P20/14 hereafter. Tests were conducted with and without geogrid reinforcement for comparison purposes, these tests are denoted as RP20/14 and UP20/14 respectively, where first letter represents the reinforcement condition and rest is applied stress level.

Figure 2 shows the induced strains in reinforced and unreinforced clay specimens during wetting-drying. Measured deformations have been converted here into strains. ε_{xt} and ε_{xb} represent horizontal strains measured at LPS positions L_T and L_B respectively. The value of ε_y is the vertical strain. Positive strain represents expansion of soil. Both specimens show similar trend of swell-shrink. However, the average expansion in geogrid-reinforced specimen is generally less than in the unreinforced specimen. The presence of geogrid reduced the average horizontal strain by 23% and the vertical strain by 17%. These results are comparable in horizontal strain but disagree with vertical strain in the wetting test results of Vessely and Wu (2002) on geosynthetic-reinforced and unreinforced clay block under free swell. During the drying process, the measured deformation indicated compression in both specimens in vertical and lateral directions. Clay shrunk more in reinforced specimen than in unreinforced specimen. This is because in

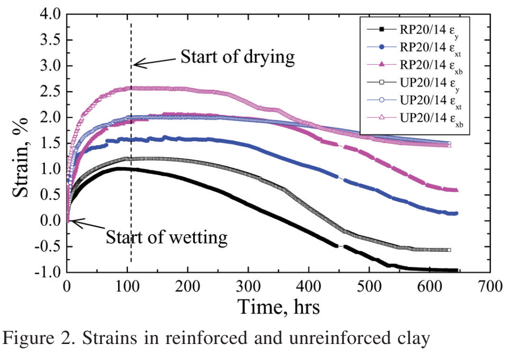

Figure 2. Strains in reinforced and unreinforced clay specimen during wetting-drying.

reinforced specimen hot air was supplied from top and bottom of specimen whereas in unreinforced specimen hot air was supplied only from bottom of specimen. Overall, geogrid reinforcement was helpful in reducing the expansion of clay during wetting; consistent with the general understanding that geogrid functions as tensile reinforcement.

Figure 3 shows the strain induced in the geogrid due to wetting-drying. As expected, geogrid strain is higher near the centerline (at S_1) than at the outer ends (S_2 and S_3). Strain gauge S_1 stopped functioning at about the end of wetting. Strains in geogrid increased during wetting and decreased during drying process. Rate of strain increment was high within a day of wetting and then showed slow rate thereafter. About 0.75% of geogrid strain has been observed as the highest value during the wetting process.

3 NUMERICAL ANALYSIS

Reinforced soil fills are compacted at prescribed moisture-density conditions. Compacted soil will usually be at an unsaturated state. Post-construction wetting-drying of expansive clays can cause vertical and lateral movements of the slopes and embankments. Alonso et al. (1990) proposed the constitutive model (also called Barcelona Basic Model, BBM) in the framework of hardening elasto-plasticity to describe the stress-strain behavior of unsaturated expansive soils. BBM extends the Modified Cam-clay Model by including suction effects. Due to space limitation, this model will not be described here; but in this study the BBM has been coded as FISH function in FLAC program to simulate mechanical loading effects at constant suction. Then, wetting effect has been decoupled from the BBM and wetting has been modeled separately with incremental form of Hooke's law (non-linear elasticity) using the following swell functions (Pathak et al. 2003):

$$\Delta\sigma_{xw} = -\lfloor \alpha_1\varepsilon_{xw} + \alpha_2\,(\varepsilon_{yw} + \varepsilon_{zw})\rfloor$$

$$\Delta\sigma_{yw} = -\lfloor \alpha_1\varepsilon_{yw} + \alpha_2\,(\varepsilon_{xw} + \varepsilon_{zw})\rfloor \quad (1)$$

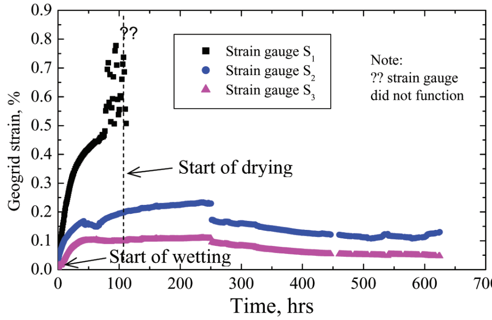

Figure 3. Geogrid strains during wetting-drying.

$$\Delta\sigma_{zw} = -\lfloor \alpha_1\varepsilon_{zw} + \alpha_2\,(\varepsilon_{xw} + \varepsilon_{yw})\rfloor$$

where,

$$\alpha_1 = K + \frac{4}{3}G \quad \text{and} \quad \alpha_2 = K - \frac{2}{3}G \quad (2)$$

K and G are bulk and shear modulus respectively. ε_{xw}, ε_{yw} and ε_{zw} are wetting-induced strains and $\Delta\sigma_{xw}$, $\Delta\sigma_{yw}$ and $\Delta\sigma_{zw}$ are wetting strain induced stresses in x-, y- and z-directions respectively. In this study, ε_{zw} is zero due to plane-strain condition. Wetting-induced strains are expressed by following logarithmic functions in terms of vertical stress (σ_y), normalized by the atmospheric pressure (p_a):

$$\varepsilon_{yw} = c_1 \log\,\{a_1(-\sigma_y/p_a)\} \quad (3)$$

$$\sigma_{xw} = c_3 \log\,\{a_3(-\,\sigma_y/p_a)\} \quad (4)$$

The parameter set a_1, c_1, a_3 and c_3 are dimensionless soil properties and determined from plane-strain compression tests of unreinforced clay carried out in this study. In the above equations, the sign convention is that compressive stresses and strains are negative.

Figure 4 shows the numerical mesh used for FLAC program to simulate the geogrid-reinforced clay specimen in vertical symmetrical half-section. The bottom boundary is fixed in both vertical and horizontal directions. The left side boundary is simulated with roller which allows the movement in vertical direction while the right side boundary is free to move with applied load boundary.

The soil properties used in the numerical simulation are as follows: K = 15 MPa, G = 3.5 MPa, a_1 = 1.863, a_3 = 0.82 and $c_1 = c_3 = -0.0272$ were used to model wetting effect. Geogrid reinforcement was modeled using two-noded linear elastic cable elements. The geogrid properties are: Young's modulus (E) = 100 MPa, tensile yield limit (yield) = 14 kN, compressive yield limit (ycomp) = 3.3 kN and geometric properties: area (A) = 0.003 m^2 and perimeter (peri) = 2 m were used in the analysis. Geogrid strength values supplied by manufacturer were reduced by half to account the removal of geogrid alternate strips from virgin geogrid. Soil-geogrid

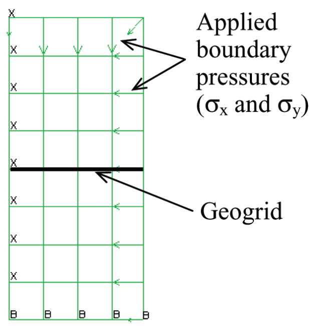

Figure 4. Numerical grid of geogrid-reinforced clay specimen.

interface behavior was modeled by using the cable grout utility in the FLAC program. Since laboratory pullout test has not been completed yet, reduced shear properties of clay were used as shear interface properties of clay-geogrid: shear stiffness (K_{bond}) = 2.34e^4 kN/m/m, cohesive strength (S_{bond}) = 10 kN/m and frictional angle (δ) =11.5°.

Initial stresses in the test specimen at its compacted condition were determined by gravity loading. Then, analysis was performed with BBM for applied incremental mechanical loading (vertical stress of 20 kPa on top boundary and horizontal stress of 14 kPa on right side boundary). The displacements determined from numerical analysis under the mechanical loading were found to be consistent with the laboratory measured values. These displacements were then set to zero before wetting simulation was activated to determine the wetting-induced deformations following the swell function.

3.1 *Results of numerical analysis*

Figure 5 shows displacement vectors of the geogrid-reinforced specimen. Soil expands both in horizontal and vertical directions. Average horizontal expansion was found to be 4.04 mm (ε_{xw} = 1.88%) and vertical expansion was 5.78 mm (ε_{yw} = 1.16%) which are comparable with the laboratory measured values. Similar expansion trend was also found in unreinforced sample; however, due to limited space result has not been shown here. In comparing this result to the unreinforced clay, geogrid reduced the horizontal expansion only in the middle area (where geogrid was placed) by about 4%. Interestingly, vertical strain has increased in reinforced clay than in unreinforced one. It is unclear at the moment if the reduced horizontal strain in reinforced clay may have attributed to this effect.

Figure 6 shows strain induced in the geogrid due to wetting (at full saturation) and mechanical loading. About 0.94% of geogrid strain was predicted due to wetting only, which is comparable with 0.75% measured during the wetting in the laboratory.

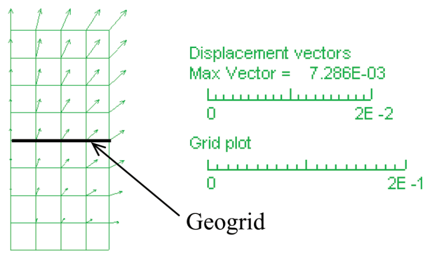

Figure 5. Displacement vectors in reinforced clay specimen due to wetting.

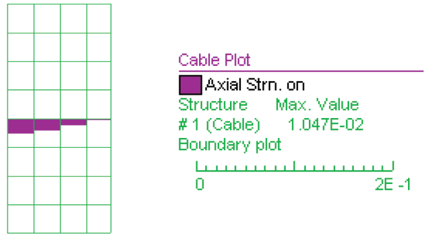

Figure 6. Strain induced in geogrid due to wetting.

4 CONCLUSIONS

Laboratory tests were performed in geogrid-reinforced and unreinforced clay under wetting-drying. A numerical analysis was also performed to simulate the wetting effect in laboratory reinforced clay specimen. Following conclusions can be drawn from this study:

- Wetting-drying induces additional strains in geogrid reinforcement and needs to be considered in the analysis and design of GRS structures using expansive clay soil.
- Geogrid helps to reduce the horizontal displacement during wetting to a small extent.
- The numerical model developed in this study was found to be reasonable in predicting the behavior of reinforced expansive clay during wetting.

REFERENCES

Al-Omari, R.R. and Hamodi, F.J. (1991). "Swelling Resistant Geogrid – A New Approach for the Treatment of Expansive Soils", Geotextiles and Geomembranes, Vol. 10, pp. 259-317.

Alonso, E.E., Gens, A. and Josa, A. (1990). "A Constitutive Model for Partially Saturated Soils", Geotechnique, Vol. 40, No. 3, pp. 405-430.

Pathak, Y.P. and Alfaro, M.C. (2005). "Behavior of Geogrid-Reinforce Clay under Wetting-Drying Cycle", Proceeding of 58th Canadian Geotechnical Conference, Saskatoon, Canada (Proceeding in CD-ROM).

Pathak, Y.P., Alfaro, M.C. and Detournay, C. (2003). "Wetting-induced Deformation of Geosynthetic Reinforced Slopes with Expansive Soils", Proceeding of 56th Canadian Geotechnical Conference, Winnipeg, Canada (Proceeding in CD-ROM).

Vessely, M.J. and Wu, J.T.H. (2002). "Feasibility of Geosynthetic Inclusion for Reducing Swelling of Expansive Soils", Transportation Research Record, Vol. 1787, pp. 42-52.